PNAS RESEARCH ARTICLE | DEVELOPMENTAL BIOLOGY

TFEB safeguards trophoblast syncytialization in humans and mice

Wanshan Zheng[a,1], Yue Zhang[a,1], Peiqun Xu[a], Zexin Wang[b], Xuan Shao[c,d,e], Chunyan Chen[a], Han Cai[a], Yinan Wang[a], Ming-an Sun[f], Wenbo Deng[a], Fan Liu[a], Jinhua Lu[a], Xueqin Zhang[a], Dunjin Cheng[g,h], Indira U. Mysorekar[i,j], Haibin Wang[a], Yan-Ling Wang[c,d,e,2], Xiaoqian Hu[b,2], and Bin Cao[a,2]

Affiliations are included on p. 12.

Edited by R. Roberts, University of Missouri, Columbia, MO; received February 29, 2024; accepted May 17, 2024

Nutrient sensing and adaptation in the placenta are essential for pregnancy viability and proper fetal growth. Our recent study demonstrated that the placenta adapts to nutrient insufficiency through mechanistic target of rapamycin (mTOR) inhibition–mediated trophoblast differentiation toward syncytiotrophoblasts (STBs), a highly specialized multinucleated trophoblast subtype mediating extensive maternal–fetal interactions. However, the underlying mechanism remains elusive. Here, we unravel the indispensable role of the mTORC1 downstream transcriptional factor TFEB in STB formation both in vitro and in vivo. TFEB deficiency significantly impaired STB differentiation in human trophoblasts and placenta organoids. Consistently, systemic or trophoblast-specific deletion of *Tfeb* compromised STB formation and placental vascular construction, leading to severe embryonic lethality. Mechanistically, TFEB conferred direct transcriptional activation of the fusogen *ERVFRD-1* in human trophoblasts and thereby promoted STB formation, independent of its canonical function as a master regulator of the autophagy-lysosomal pathway. Moreover, we demonstrated that TFEB directed the trophoblast syncytialization response driven by mTOR complex 1 (mTORC1) signaling. TFEB expression positively correlated with the reinforced trophoblast syncytialization in human fetal growth–restricted placentas exhibiting suppressed mTORC1 activity. Our findings substantiate that the TFEB-fusogen axis ensures proper STB formation during placenta development and under nutrient stress, shedding light on TFEB as a mechanistic link between nutrient-sensing machinery and trophoblast differentiation.

syncytiotrophoblast | TFEB | ERVFRD-1 | human trophoblast stem cell | fetal growth restriction

Significance

The formation of multinucleated syncytiotrophoblast (STB) through cell fusion of cytotrophoblast, also termed syncytialization, ensures the proper placental structure and functions. Nutrient insufficiency and inactivation of the mechanistic target of rapamycin complex 1 (mTORC1) in trophoblasts have been shown to enhance STB formation; however, the underlying mechanism remains elusive. Here, we showed that the deficiency of a mTORC1 downstream transcriptional factor, TFEB, significantly impaired STB formation in human trophoblasts and knock-out mice. TFEB conferred direct transcriptional activation of the fusogen *ERVFRD-1* and thereby promoted trophoblast syncytialization. Additionally, TFEB expression positively correlated with the reinforced trophoblast syncytialization in human fetal growth restriction placentas with suppressed mTORC1 activity. Our findings substantiate that the TFEB-fusogen axis safeguards proper STB formation during placenta development.

The placenta is a complex organ that sustains successful pregnancy and embryonic development throughout gestation by facilitating critical functions, ranging from nutrient and gas transport to hormone production, immune tolerance, and pathogen restriction. To fulfill these diverse functions, human trophoblast stem cells (hTSCs) give rise to highly specialized trophoblast lineages, including cytotrophoblast (CTB), syncytiotrophoblast (STB), and extravillous trophoblast (EVT) (1, 2). STBs which are bathed in maternal blood are the largest multinucleated epithelial cells in humans. They line the placental villi and constitute a continuous maternal–fetal interface that primarily governs the endocrine, nutritive, and protective functions of the placenta (3, 4). Emerging evidence suggests that the STB not only simply facilitates nutrients traversing the placental barrier to the fetus but also integrates placental growth and function in response to maternal and fetal nutrient signals (5). STBs are formed and replenished through the cell fusion of hTSC-featured mononucleated CTBs, also termed trophoblast syncytialization. Aberrant STB formation disrupts structural and functional homeostasis of the placenta, which is associated with devastating pregnancy complications such as preeclampsia and fetal growth restriction (FGR) (6, 7).

To form syncytia, highly proliferative CTBs first exit the cell cycle and subsequently undergo transcriptional reprogramming to active genes critical for trophoblast fusion and STB formation, including transcriptional factors and fusogens (8, 9). SYNCYTIN1 (encoded by endogenous retrovirus group W envelope member 1, *ERVW-1*) and SYNCYTIN2 (encoded by endogenous retrovirus group FRD member 1, *ERVFRD-1*), the bona fide fusogens in the human placenta, bind to their corresponding receptors, thereby spanning opposing plasma membranes of adjacent fusion-competent trophoblasts and promoting membrane fusion (10–12). Trophoblast syncytialization is fine-tuned by a comprehensive interplay of molecular and cellular events, including cytoskeletal

Competing interest statement: I.U.M. serves on the scientific advisory board of Luca Biologics.

This article is a PNAS Direct Submission.

[1]W.Z. and Y.Z. contributed equally to this work.

[2]To whom correspondence may be addressed. Email: wangyl@ioz.ac.cn, xqhu@xmu.edu.cn, or caobin19@xmu.edu.cn.

This article contains supporting information online at https://www.pnas.org/lookup/suppl/doi:10.1073/pnas.2404062121/-/DCSupplemental.

Published July 5, 2024.

and membrane remodeling, transcriptional program rewiring, epigenetic regulation, and alteration of signaling pathways (13–16). Our previous study revealed that amino acid deprivation and inactivation of the mechanistic target of rapamycin complex 1 (mTORC1) in trophoblasts significantly enhanced syncytium formation and the corresponding nutrient uptake through macropinocytosis, which allows the placenta to efficiently adapt to nutrient insufficiency and ensure fetal growth during pregnancy (17). However, the mechanisms underlying this nutritional regulation of trophoblast syncytialization remain to be explored.

Transcriptional factor EB (TFEB), a basic helix–loop–helix leucine zipper transcription factor, functions as a master regulator of autophagy and lysosomal biogenesis, which binds directly to the CLEAR (Coordinated Lysosomal Expression and Regulation) motifs of target genes and drives gene expression in response to nutritional and lysosomal stress (18). The activity of TFEB is tightly controlled by nutrient availability and mTOR signaling. In nutrient-rich conditions, the active mTORC1 phosphorylates TFEB at the surface of lysosomes, thus retaining TFEB in the cytoplasm; Upon nutrient deprivation, TFEB is dephosphorylated and translocated to the nucleus, driving the transcription of its target genes (19). Emerging evidence highlights the importance of TFEB in diverse physiological events, while dysregulated TFEB activity contributes to the pathogenesis of several diseases, including cancers, infections, neurodegenerative diseases, metabolic disorders, and inflammatory diseases (20).

In this study, we identify an indispensable function of TFEB in trophoblast syncytialization. Through a combination of loss- and gain-of-function assays, we demonstrated that endogenous TFEB expression is necessary for proper syncytialization in the trophoblast cells and placenta organoids. Mechanistically, we profiled specific TFEB target genes in trophoblasts and identified that TFEB drives transcriptional activation of the fusogen *ERVFRD-1,* instead of the known autophagic and lysosomal genes, thereby promoting trophoblast cell fusion. In keeping with these findings, genetic deletion of *Tfeb* in trophoblasts disabled STB formation in mouse placentas, leading to severe placental dysfunction and embryonic lethality. Furthermore, TFEB facilitates the STB formation driven by mTORC1 inhibition, which is associated with excessive trophoblast syncytialization in the FGR placentas.

Results

Dynamic Changes in TFEB Expression during Trophoblast Syncytialization. We have recently characterized augmented trophoblast syncytialization in response to mTORC1 inhibition functions as an adaptation strategy to counteract the challenge of nutrient scarcity during pregnancy (17). However, the mechanistic link between mTORC1 suppression and syncytium formation remains unclear. Thus, we initially utilized publicly available RNA-seq datasets to evaluate the expression of mTOR downstream targets in CTBs versus STBs (21). We noticed that representative mTOR downstream genes (i.e., *RPS6KB1*, *TFEB*, *EIF4E*, *HIF1A*, *LPIN1,* and *GRB10*) were more abundantly expressed in primary CTBs and hTSCs relative to their corresponding differentiated STBs (*SI Appendix,* Fig. S1*A*). Herein, we focused on the TFEB, which is tightly regulated by mTORC1 signaling and has recently been proposed as a potential STB regulator (22).

To explore the significance of TFEB in trophoblast cell fate specification, we illustrated the spatial expression of TFEB in the human placenta. Immunofluorescent staining for TFEB, along with canonical markers of different trophoblast subtypes (CDH1 for CTB, hCGβ for STB, HLA-G for EVT), revealed that TFEB expression was mainly restricted to CTBs compared with STBs and EVTs in the first-trimester placenta (Fig. 1*A* and *SI Appendix,* Fig. S1*B*). To further verify the TFEB expression pattern in different trophoblasts, we utilized the hTSC-derived human trophoblast organoid (TO), which forms a self-organized spheroid structure with sustained mononucleated CTBs at the surface and spontaneously differentiated STBs residing in the interior. We observed that TFEB expression was confined to CDH1 positive CTBs outlining the surface of TOs, whereas TFEB was nearly undetectable in the interior STBs (Fig. 1*B*).

In addition, we characterized the dynamic changes in TFEB expression during trophoblast syncytialization using three trophoblast fusion models: primary human trophoblasts (PHTs), the BeWo trophoblast cell line, and hTSCs (*SI Appendix,* Fig. S1*C*). Mononucleated PHTs spontaneously underwent fusion within 24 to 48 h after plating, as indicated by an increased hCGβ expression (Fig. 1*C*). Western blot showed that unfused PHTs (0 h) displayed a higher abundance of TFEB expression, which markedly declined as cell fusion proceeded over time (Fig. 1*C*). In the second model, trophoblast fusion was progressively induced by continuous forskolin (FSK) treatment in BeWo (*SI Appendix,* Fig. S1*C*), verified by elevated expression of representative STB markers [including *ERVW-1*, *ERVFRD-1*, glial cells missing transcription factor 1 (*GCM1*), and *hCG*] and a striking decrease in CDH1 expression (*SI Appendix,* Fig. S1*D*). Accordingly, we observed a significant decrease in both the RNA and protein levels of TFEB, concomitant with the advancing formation of multinucleated BeWo cells (Fig. 1 *D* and *E* and *SI Appendix,* Fig. S1*E*). Given the advantages of hTSCs in studying human trophoblast differentiation, we finally evaluated TFEB expression in hTSCs and the corresponding hTSC-derived STBs. As expected, the abundant TFEB expression was significantly down-regulated once hTSCs underwent syncytialization at 72 to 96 h, coinciding with decreased TP63 expression (a hTSC marker) and the upregulation of hCGβ (Fig. 1 *F* and *G*). Taken together, the TFEB expression pattern in CTBs and STBs suggests a potential regulatory role of TFEB in the process of trophoblast syncytialization.

TFEB Sustains Trophoblast Syncytialization. To elucidate the function of TFEB in trophoblast syncytialization, we initially conducted siRNA knockdown (KD) of *TFEB* in BeWo, as verified by qPCR and immunoblot (*SI Appendix,* Fig. S2*A* and Fig. 2*C*). Notably, staining for CDH1 and hCG showed that *TFEB* KD cells failed to efficiently form multinucleated syncytia upon FSK stimulation (Fig. 2 *A* and *B* and *SI Appendix,* Fig. S2 *B* and *C*). Consistently, western blot and qPCR of markers for CTB and STB further supported our findings that TFEB deficiency significantly abolished STB formation in BeWo (Fig. 2*C* and *SI Appendix,* Fig. S2*D*). Furthermore, hCG secretion, a hallmark of functional STB, was significantly suppressed in the supernatant of KD cells (Fig. 2*D*). To corroborate our findings, we constructed *TFEB* knockout (KO) BeWo clones using CRISPR-Cas9 genome editing technology (*SI Appendix,* Fig. S2*E*). In line with the above results, cell fusion was further impaired in *TFEB* KO cells, as assessed by immunofluorescent staining, western blot, and hCG enzyme-linked immunosorbent assay (ELISA) measurement (*SI Appendix,* Fig. S2 *F–H*). In addition, transcriptome analysis revealed substantially altered transcriptome signatures in *TFEB* KO cells associated with compromised trophoblast fusion, including dramatically repressed STB genes and the enrichment of down-regulated differentially expressed genes (DEGs) in GO terms related to placenta development, cell–cell junction, and Wnt signaling, the pathways proven to play critical roles in trophoblast syncytialization (*SI Appendix,* Fig. S2 *I–K*).

To complement our observation that TFEB deficiency impaired trophoblast fusion, we next investigated whether TFEB overexpression

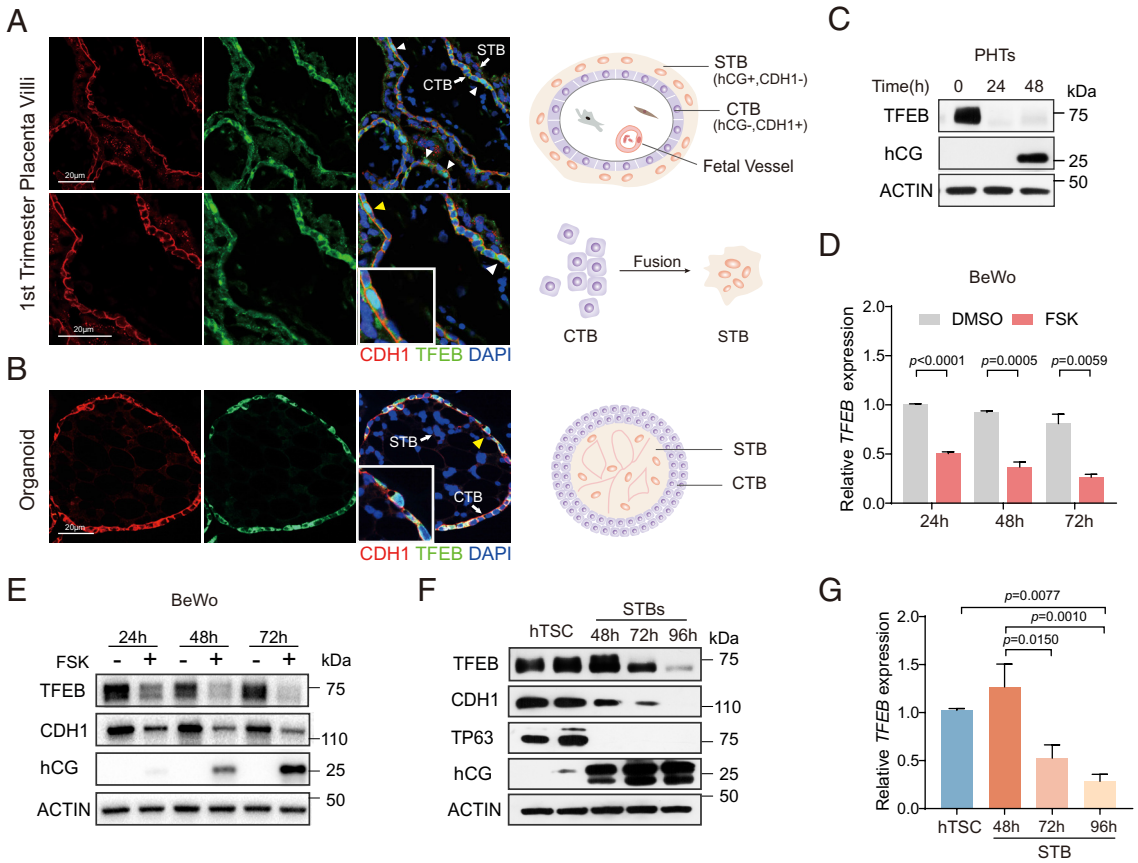

Fig. 1. Dynamic changes in TFEB expression during trophoblast syncytialization. (*A* and *B*) Representative TFEB immunostaining in first-trimester placentas (*A*) and TOs (*B*). Arrowheads, the nuclear expression of TFEB. Yellow arrowheads show the area with higher magnification displayed as inserts. *Right* panels, schematic illustrations of first-trimester placental villi and TOs. (*C*) Western blot shows the expression of TFEB and hCGβ in PHTs, which spontaneously fuse into STBs after 24 h culture. (*D*) qPCR analysis of *TFEB* in Dimethyl sulfoxide (DMSO) or FSK-treated BeWo cells at the indicated time points of syncytialization. n = 3. (*E*) Immunoblot analysis of TFEB, CDH1, and hCGβ in BeWo cells treated with DMSO or FSK for 24 h, 48 h, and 72 h. (*F*) Immunoblot of TFEB, CDH1, TP63, and hCGβ in hTSCs and hTSCs-derived STBs (48 h, 72 h, and 96 h). (*G*) Quantitative gene expression analysis of *TFEB* during dynamic differentiation of STBs from hTSCs. (n = 5 for 96 h and n = 3 for others).

promotes trophoblast syncytialization. Remarkably, approximately 40% of BeWo cells with ectopic TFEB overexpression fused at 36 h post-FSK treatment, whereas the corresponding fusion index in control cells was less than 10% (Fig. 2 *E* and *F* and *SI Appendix*, Fig. S2*L*), suggesting that TFEB overexpression significantly potentiates the progression of trophoblast syncytialization. Taken together, these findings highlight that TFEB is indispensable for trophoblast cell fusion.

TFEB Is Necessary for hTSC Differentiation into STB, but Not for EVT Differentiation. The aforementioned findings in the trophoblast cell line prompted us to further examine whether TFEB is also essential for hTSCs differentiation into trophoblast subtypes, which mainly follows the STB and EVT differentiation routes. To this end, we generated *TFEB* KO hTSCs clones as validated by western blot and Sanger sequencing (*SI Appendix*, Fig. S3 *A* and *B*). First, we confirmed that TFEB-depleted hTSCs displayed a normal morphology identical to the controls (*SI Appendix*, Fig. S3*C*), and sustained stemness as evidenced by the indistinguishable expression of hTSC hallmarks (TP63, TEAD4, and GATA3) (*SI Appendix*, Fig. S3 *A* and *D*). Akin to *TFEB* KO BeWo cells, disruption of TFEB abrogated STB differentiation in 2D hTSCs culture (Fig. 2 *G* and *H*). Accordingly, STB markers (including SDC1, GCM1, ERVFRD-1, and hCGβ) were robustly repressed in the *TFEB* KO hTSCs cultured under the STB differentiation condition (Fig. 2 *I* and *J*). Next, we further analyzed the impact of TFEB on STB differentiation in 3D TOs, where STB spontaneously forms independent of exogenous treatment. Control hTSCs cultivated in 3D formed typical architectures of well-organized TOs with SDC1-positive STBs within the organoid cavity (Fig. 2*K* and *SI Appendix*, Fig. S3 *E–G*). In contrast, the interior of *TFEB* KO organoids was predominantly occupied by CDH1+ CTBs instead of well-differentiated STBs (Fig. 2*K* and *SI Appendix*, Fig. S3 *E–G*). Nevertheless, this is not due to differences in cell growth upon TFEB deletion, as the KO organoids retained normal sizes (*SI Appendix*, Fig. S3*H*). We subsequently asked whether the regulatory effect of TFEB on STB differentiation relies on its nuclear translocation and function. Indeed, the exogenous overexpression of wild-type (WT) TFEB or a constitutively active form of TFEB (TFEB-S211A) significantly rescued the impaired syncytialization phenotype, whereas the inactivation TFEB mutant with the deletion of nuclear localization signal (TFEB-ΔNLS) retained in the cytoplasm did not ameliorate cell fusion defects in the *TFEB* KO hTSCs (Fig. 2 *L* and *M*). Overall, these data suggest that TFEB is an essential regulator of STB differentiation, prominently relying on its nuclear localization.

To investigate whether TFEB also affects EVT differentiation, we subjected *TFEB* KO hTSCs to the EVT differentiation medium and found that they were able to form typical spindle-shaped HLA-G positive EVTs (*SI Appendix*, Fig. S3*I*). Additionally, the expression of EVT markers (HLA-G, PLAC8, ITGA1, MCAM, and MMP2) showed no difference between *TFEB* KO and control hTSC-derived EVTs (*SI Appendix*, Fig. S3 *J* and *K*). In line with the observation from 2D EVT cultures, *TFEB*-depleted TOs also presented mesenchymal spindle-shaped EVT outgrowth in response to the EVT^{3D} condition (*SI Appendix*, Fig. S3*L*). In

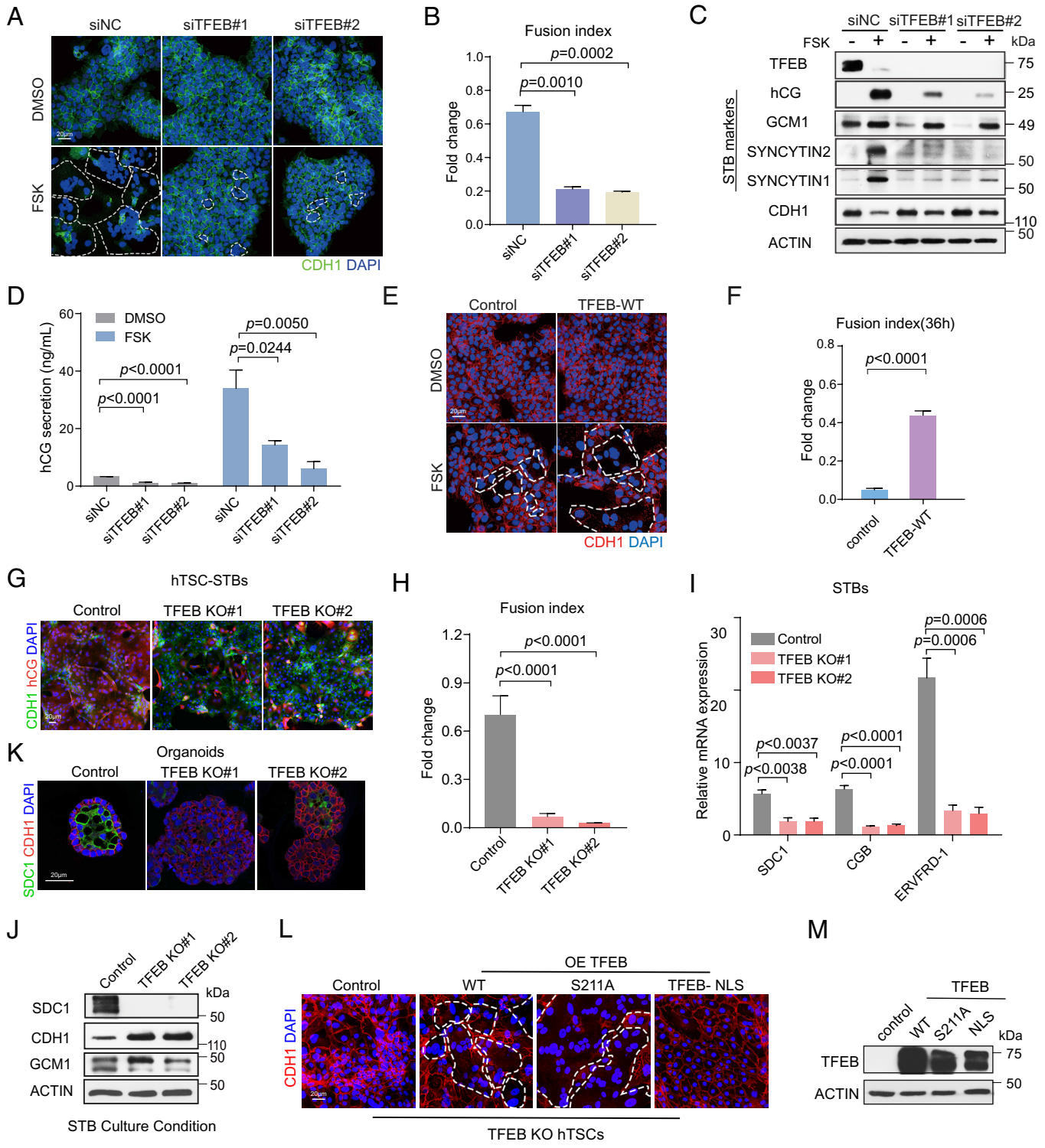

Fig. 2. TFEB ensures proper trophoblast syncytialization. (*A*) Representative immunofluorescence for CDH1 in TFEB KD and control BeWo cells subjected to either DMSO or FSK for 60 h. (*B*) Quantification of trophoblast syncytialization in BeWo cells with the indicated siRNA treatments using fusion index. At least 15 confocal images were randomly selected for each group. (*C*) Western blots of TFEB and STB genes in the indicated BeWo cells. (*D*) ELISA detection of hCG secretion in culture media. n = 3. (*E* and *F*) Representative CDH1 immunofluorescent staining (*E*) and the corresponding calculation of STBs (*F*) show the syncytialization efficiency in BeWo cells with or without exogenous overexpression of WT-TFEB. Control, empty vector. n = 15 from three independent experiments. (*G* and *H*) Immunofluorescence images showing the syncytialization capacity of the control versus TFEB KO hTSCs at the 96 h differentiation time point (*G*). The corresponding fusion index is shown in (*H*). n = 9 from three independent experiments. (*I* and *J*) mRNA (*I*) and protein (*J*) expression of STB markers in the indicated hTSCs (cultured in the STBs culture medium for 96 h). n = 3 in (*I*). (*K*) Immunofluorescence images of CDH1 and SDC1 showing syncytium formation in 3D TOs. (*L* and *M*) Immunofluorescence staining of CDH1 in TFEB KO hTSCs stably overexpressing TFEB-WT, TFEB-S211A, or TFEB-ΔNLS (FSK, 72 h). Control, empty vector. Overexpression was confirmed by immunoblot in (*M*). In panels (*A*), (*E*), and (*L*), CDH1 staining delineates boundaries between BeWo cells; The white dashed lines outline multinucleated STBs.

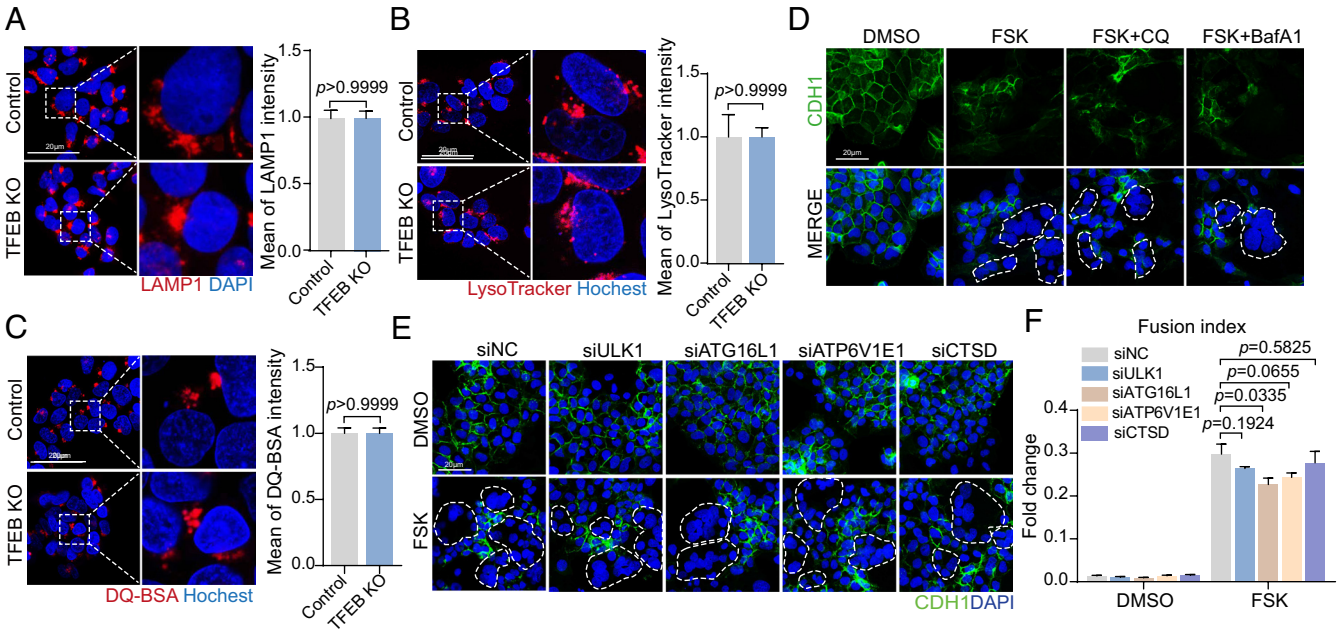

Fig. 3. Impaired trophoblast fusion induced by TFEB deficiency is independent of the autophagy-lysosomal pathway. (*A–C*) Representative confocal imaging for LAMP1 (*A,* n = 3), LysoTracker (*B,* n = 4), and DQ-BSA (*C,* n = 3). The corresponding quantification was shown in the *Right* panels. (*D*) Representative immunofluorescence images of CDH1 in BeWo cells with 48 h treatment of DMSO, FSK, or FSK supplemented with 5 mM CQ or 25 nM BafA1. Representative STBs are outlined with white dashed lines. (*E* and *F*) Immunostainings for CDH1 (*E*) and the corresponding quantification of trophoblast fusion (48 h FSK treatment) (*F*) in BeWo cells transfected with siRNA targeting the indicated autophagic or lysosomal genes. n = 5.

summary, TFEB is necessary for STB differentiation from hTSCs but is dispensable for EVT lineage specification.

TFEB Facilities the STB Formation Driven by mTORC1 Signaling. Our previous study demonstrates that mTORC1 inhibition is a determinant of reinforced trophoblast syncytialization during pregnancy (17). Here, we observed that mTORC1 suppression by rapamycin treatment remarkedly promoted the nuclear sequestration of TFEB (*SI Appendix,* Fig. S4*A*). Thus, we simultaneously modulated the activity of mTORC1 and TFEB to explore whether TFEB mediates the STB formation driven by the mTORC1 nutrient signaling. Trophoblast fusion assay revealed that rapamycin-induced excessive STB formation is completely blunted upon TFEB depletion (*SI Appendix,* Fig. S4*B*). Consistently, the treatment of trehalose, a TFEB agonist promoting TFEB nuclear translocation, successfully rescued the impaired STB differentiation in TOs induced by mTORC1 activator MYH1485 (*SI Appendix,* Fig. S4 *C* and *D*). These findings together suggest that TFEB not only endogenously sustains STB differentiation capacity but also directs the trophoblast syncytialization response driven by mTORC1 signaling and nutrient stress.

TFEB-Mediated Trophoblast Syncytialization Is Independent of the Autophagy Lysosomal Pathway. Canonically, TFEB has been shown to directly bind to CLEAR elements, thereby orchestrating the expression of genes essential for the autophagy pathway and lysosomal biogenesis (*SI Appendix,* Fig. S5*A*) (23). Thus, we speculated whether TFEB governs trophoblast syncytialization through transcriptional regulation of lysosomal and autophagic genes. To explore this, we examined the expression of genes related to lysosomal biogenesis and autophagy during STB formation (*SI Appendix,* Fig. S5 *B–D*). We found certain known TFEB target genes of the autolysosomal pathway, such as P62 and ATG16L1, were indeed down-regulated in *TFEB* KO cells, whereas the expression of other autophagy or lysosomal genes (including ATG14, BECLIN1, LAMP1, and CTSD) did not alter both at steady state or following FSK treatment (*SI Appendix,* Fig. S5 *B–D*). Next, we investigated whether the TFEB deletion in trophoblasts affects lysosome biogenesis and function using multiple assays. LAMP1 staining revealed that TFEB deficiency did not change the number of lysosomes (Fig. 3*A*). Likewise, the fluorescence intensity of LysoTracker, an acidotropic probe indicating lysosomal acidification, was similar in *TFEB* KO cells versus control cells (Fig. 3*B*). Simultaneously, we analyzed lysosomal function using DQ-BSA, a dye that indicates active proteolysis in lysosomes. The DQ-BSA intensity revealed that lysosomal activity sustains upon TFEB deletion (Fig. 3*C*). Furthermore, we assessed the impact of TFEB on autophagic activity and found that *TFEB* KO cells harbored a similar amount of LC3 puncta compared to control cells (*SI Appendix,* Fig. S5*E*). In summary, TFEB deficiency did not affect the number, acidity, and proteolysis function of lysosomes, as well as autophagic activity in trophoblasts. These results imply that compromised STB formation in *TFEB* KO cells might not be attributed to attenuated autophagic activity or lysosomal dysfunction. To further support this hypothesis, we blocked autophagic or lysosomal activity through pharmacological treatments of lysosome inhibitors (CQ or BafA1) or siRNAs targeting critical autophagy and lysosomal genes. Cell fusion assay revealed that blocking autolysosomal pathways is not sufficient to recapitulate the impaired syncytialization phenotype in *TFEB* KO cells (Fig. 3 *D–F* and *SI Appendix,* Fig. S5*F*). Our evidence suggests that TFEB appears to regulate trophoblast syncytialization through a mechanism independent of the autolysosomal pathway.

Identification of ERVFRD-1 As a Target Gene of TFEB Responsible for Guarding Trophoblast Syncytialization. To pinpoint the putative TFEB target genes responsible for trophoblast syncytialization, we conducted RNA-seq and genome-wide TFEB chromatin immunoprecipitation followed by sequencing (ChIP-seq) analysis. 408 genes conceiving TFEB binding within their corresponding transcription start site (TSS) were identified by TFEB ChIP-seq. We

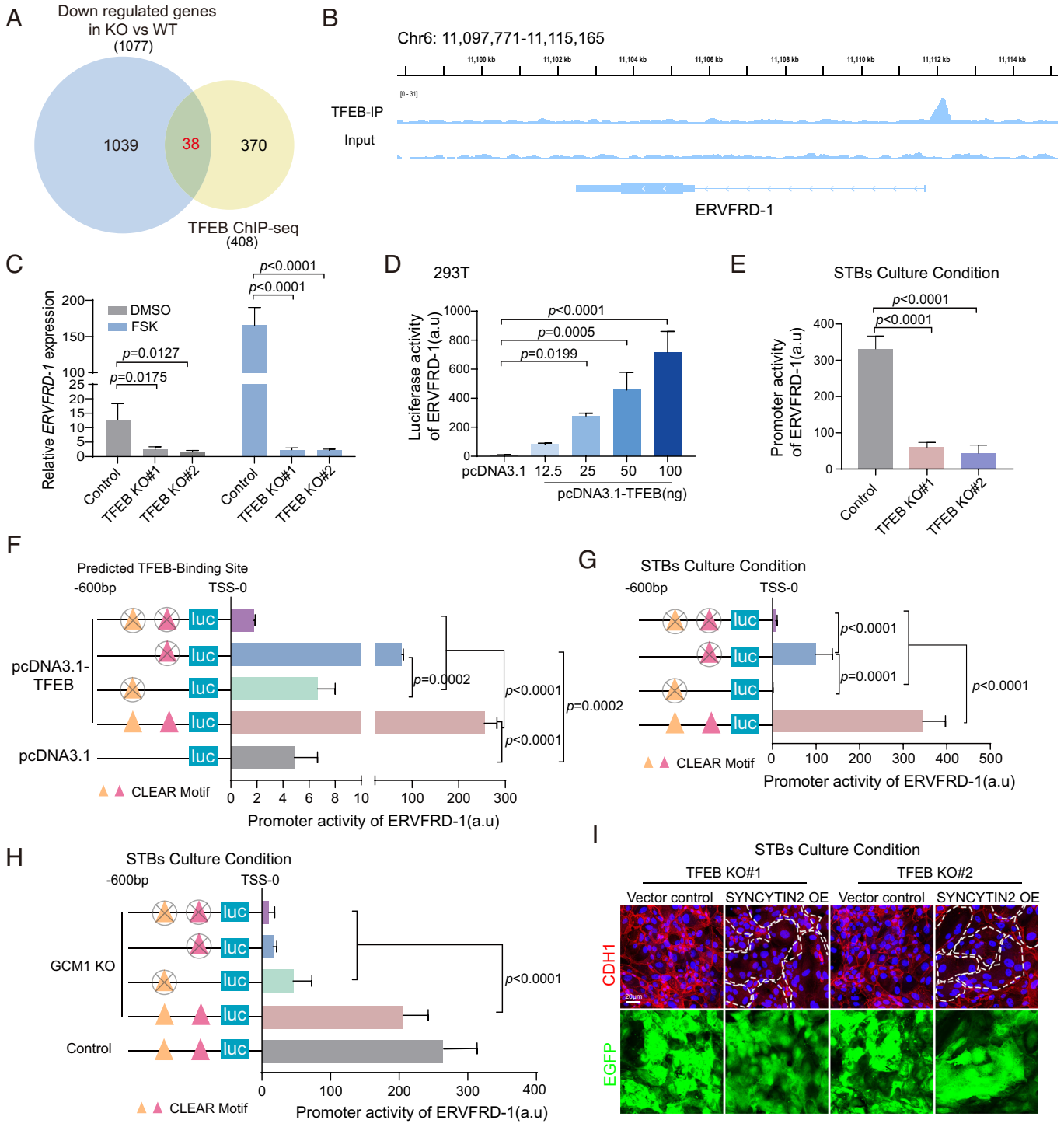

Fig. 4. ERVFRD-1 is the direct target gene of TFEB responsible for governing STB formation. (*A*) Venn diagram depicting putative TFEB target genes by intersecting genes identified by TFEB ChIP-seq with down-regulated genes in TFEB KO BeWo cells. (*B*) Integrative Genomics Viewer track of TFEB binding near the predicted ERVFRD-1 promoter. (*C*) RT-qPCR analysis of *ERVFRD-1* in TFEB KO cell lines with or without FSK treatment. n = 3. (*D–H*) Dual-luciferase reporter assays were conducted in HEK293T (*D* and *F*) or STBs (*E*,*G*, and *H*). WT (*D* and *E*) or truncated (*F–H*) ERVFRD-1 promoter reporter plasmids were introduced into the HEK293T or STBs. The promoter activities of *ERVFRD-1* in HEK293T were evaluated in response to different dosages of TFEB overexpression (*D*, n = 3). The activities of *ERVFRD-1* promoters in control, TFEB KO#1, and TFEB KO#2 STBs were assessed after 72 h differentiation (*E*, n = 3). Similarly, the WT or mutant (with single or double TFEB binding sites deletion) *ERVFRD-1* promoter activities in HEK293T (*F*, n = 3), STBs (*G*, n = 5), or GCM1 KO STBs (*H*, n = 3) were determined. (*I*) Immunofluorescence images of CDH1 in TFEB KO hTSCs upon reexpressing exogenous SYNCYTIN2. Vector control, empty pCDH-EGFP plasmid. Overexpression efficiency was validated by the EGFP immunofluorescence in the corresponding lower panels.

specifically overlapped the down-regulated genes in *TFEB* KO cells with the genes exhibiting TFEB binding enrichment, which gave rise to a cluster of 38 potential TFEB downstream targets (Fig. 4*A* and *SI Appendix*, Fig. S6*A*). Among these genes, we observed previously established TFEB targets in other biological systems (i.e., *BHLHE40*, *SQSTM1*, *RRAGC*, *PPT1*, *UAP1L1*, and *HMOX1*) (24–27) (*SI Appendix*, Fig. S6 *A* and *B*), proving the robustness of our sequencing data. Intriguingly, we observed the enrichment of TFEB binding in the promoter region of the *ERVFRD-1* gene (Fig. 4*B*), a well-characterized fusogen facilitating human

trophoblast syncytialization (8, 28), which led us to hypothesize that TFEB might directly regulate the transcription of *ERVFRD-1* in human trophoblasts. Notably, unlike *ERVFRD-1*, we did not observe TFEB binding at the promoters of *ERVW-1*, *ERVV-1*, or *ERVV-2* (*SI Appendix,* Fig. S6*B*), highlighting the specificity of TFEB-mediated transcriptional regulation on ERVFRD-1. Therefore, we next compared the transcriptional changes of *ERVFRD-1* upon TFEB deletion at steady state or after FSK stimulation. The qPCR data illustrated a significant attenuation of *ERVFRD-1* transcription after TFEB loss in trophoblasts (Fig. 4*C* and *SI Appendix*, Fig. S6*D*), whereas the overexpression of WT-TFEB and TFEB-S211A significantly potentiated *ERVFRD-1* expression (*SI Appendix,* Fig. S6*C*).

To further verify that *ERVFRD-1* is a direct transcriptional target of TFEB, we transfected 293T cells with the predicted *ERVFRD-1* promoter sequence and evaluated the luciferase activity in response to exogenous TFEB. The luciferase assay data revealed that TFEB overexpression induced a pronounced and dose-dependent increase in the promoter activity of *ERVFRD-1* (Fig. 4*D*). Consistently, *TFEB* KO STBs displayed an extremely lower luciferase intensity compared with the WT controls (Fig. 4*E*). TFEB has previously been shown to directly bind to the CLEAR element (*SI Appendix,* Fig. S6*E*), thereby driving the transcription of corresponding genes (26). Bioinformatics analysis on ChIP-sequencing data revealed two typical CLEAR motif sequences, the proximal and distal binding sites, within the *ERVFRD-1* promoter. The combined deletion of both sequences completely abolished the TFEB-induced transcriptional activation (Fig. 4*F*). Additionally, a more substantial decline in luciferase intensity was observed in the distal mutant promoter, compared with the one carrying a truncation of the proximal binding site (Fig. 4*F*). These results suggest that the distal CLEAR motif upstream of *ERVFRD-1* exhibits more potent activity in transcriptional induction. Consistent results were also observed in hTSCs (Fig. 4*G*). Altogether, these data indicate that TFEB promotes *ERVFRD-1* transcription through direct binding to the upstream CLEAR motifs.

Given that GCM1 could regulate *ERVFRD-1* expression (29), we investigated the relative contributions of GCM1 and TFEB to the transcriptional induction of *ERVFRD-1*. First, we examined the regulatory effect of TFEB on GCM1 expression and vice versa. RNA-seq data revealed a robust upregulation of GCM1 in *TFEB* KO cells treated with FSK, implying that TFEB does not affect GCM1 expression (*SI Appendix,* Fig. S2*J*). In addition, we employed CRISPR-Cas9 engineering to delete GCM1 in BeWo cells (*SI Appendix,* Fig. S6 *G* and *H*). qPCR results showed a comparable TFEB level in *GCM1* KO cells compared with controls (*SI Appendix,* Fig. S6*I*). These findings together imply no reciprocal regulation between GCM1 and TFEB at the transcriptional level. Furthermore, we demonstrated that endogenous GCM1 depletion was not sufficient to suppress the induction of *ERVFRD-1* by FSK treatment, which is further supported by the observation that full-length TFEB could successfully activate *ERVFRD-1* expression in the absence of GCM1 (Fig. 4*H* and *SI Appendix*, Fig. S6 *D* and *F*). Consistently, overexpression of GCM1 failed to adequately restore the diminished *ERVFRD-1* expression in *TFEB* KO cell lines (*SI Appendix,* Fig. S6*J*). In summary, our data suggest that TFEB acts on *ERVFRD-1* expression independently of GCM1.

We next ascertained whether genetic reestablishing *ERVFRD-1* expression could sufficiently reverse the syncytialization defects induced by TFEB deficiency. We transfected *TFEB* KO hTSC lines with exogenous SYNCYTIN2 and assessed the capacity of trophoblast fusion. Intriguingly, we found that restored SYNCYTIN2 expression effectively rescued the phenotypes of compromised trophoblast syncytialization (Fig. 4*I*), providing strong evidence that *ERVFRD-1* is the definitive TFEB target gene responsible for guarding human trophoblast syncytialization in vitro.

Loss of Tfeb in Mice Dampens Normal Placental Development. To elucidate the in vivo functional significance of Tfeb, we first generated and analyzed mice globally null for *Tfeb* (hereafter referred to as *Tfeb*$^{-/-}$). In line with the embryonic lethality phenotype in the *Tfeb*$^{-/-}$ attributed to vascularization defects (30), we observed embryonic demise of the *Tfeb*$^{-/-}$ fetus at E10.5 to E11.5 with improper placental development. To delineate detailed placental defects caused by *Tfeb* deletion, we performed histological analyses of both *Tfeb*$^{+/+}$and *Tfeb*$^{-/-}$ placentas between E8.5 and E11.5 (Fig. 5*B* and *SI Appendix,* Fig. S7*A*). The mature mouse placenta is mainly composed of three distinct trophoblast layers, including trophoblast giant cell (TGC) layer, junctional zone [with spongiotrophoblast (SpT) and glycogen trophoblast (GlyT)] and labyrinth, among which the labyrinth layer predominantly facilitates nutrient and gas exchange between the mother and fetus (Fig. 5*A*). E11.5 *Tfeb*$^{-/-}$ placenta exhibited a thinner labyrinth with malformation of placental vasculatures, shown by significantly diminished fetal blood vessels containing primitive nucleated erythrocytes (Fig. 5*B*) and disorganized endothelium of fetal blood vessels (Fig. 5*C*). In contrast to the labyrinth, the overall structure and marker expression of the TGC layer and junctional zone sustained in the mutant placentas (*SI Appendix,* Fig. S7 *B* and *C*). At the onset of labyrinth formation around E8.5, the allantois attaches and fuses with the chorion, triggering fetal blood vessels to branch and invaginate into the chorionic trophoblasts. This process subsequently gives rise to fetal capillaries, separated from maternal sinusoids by a layer of mononuclear trophoblasts and two layers of STBs, termed STB layer I (SynT-I) and STB layer II (SynT-II) respectively (Fig. 5*A*) (31). We observed that chorioallantoic attachment at E8.5 and the initiation of fetal vessel branching at E9.5 in *Tfeb*$^{-/-}$ appeared normal (*SI Appendix,* Fig. S7*A*), which implies that the labyrinth defects caused by Tfeb deficiency at E11.5 are likely attributed to the aberrant progression of branching morphogenesis and vascularization in the chorionic plate at later stages.

Trophoblast-Specific TFEB KO Mice Phenocopy *Tfeb*$^{-/-}$ Mice. Since the maturation of placental vasculatures is tightly orchestrated with trophoblast differentiation, we next evaluated detailed trophoblast phenotypes within the labyrinth. Interestingly, we noted densely packed patches of trophoblasts in the *Tfeb*$^{-/-}$ labyrinth at the expense of fetal capillary spaces by immunofluorescent staining of a trophoblast marker pan-Cytokeratin (pan-CK) (Fig. 5*D*), which led us to speculate that the labyrinth abnormality in *Tfeb*$^{-/-}$ placentas primarily results from impaired trophoblast differentiation. To test this hypothesis, we first leveraged the recent single nuclei RNA sequencing (snRNA-seq) data of mouse placenta to characterize *Tfeb* expression in different cell types in WT placentas (32). Notably, snRNA-seq analysis verified that *Tfeb* was predominantly expressed in trophoblasts but scarcely in endothelium or other cell types at the maternal–fetal interface (Fig. 5*E*). Concordantly, immunohistochemistry staining further confirmed the exclusive Tfeb expression pattern in labyrinth trophoblasts from E8.5 to E11.5 (Fig. 5*F*). Specifically, Tfeb expression was localized to the distal side of the chorion plate at the chorioallantoic attachment and fusion stage (E8.5), shifting to the trophoblasts covering the tips of the chorionic branches elongate at E9.5 and becoming ubiquitous in labyrinth trophoblasts at E11.5 (Fig. 5*F*). However, Tfeb expression in the endothelium lining

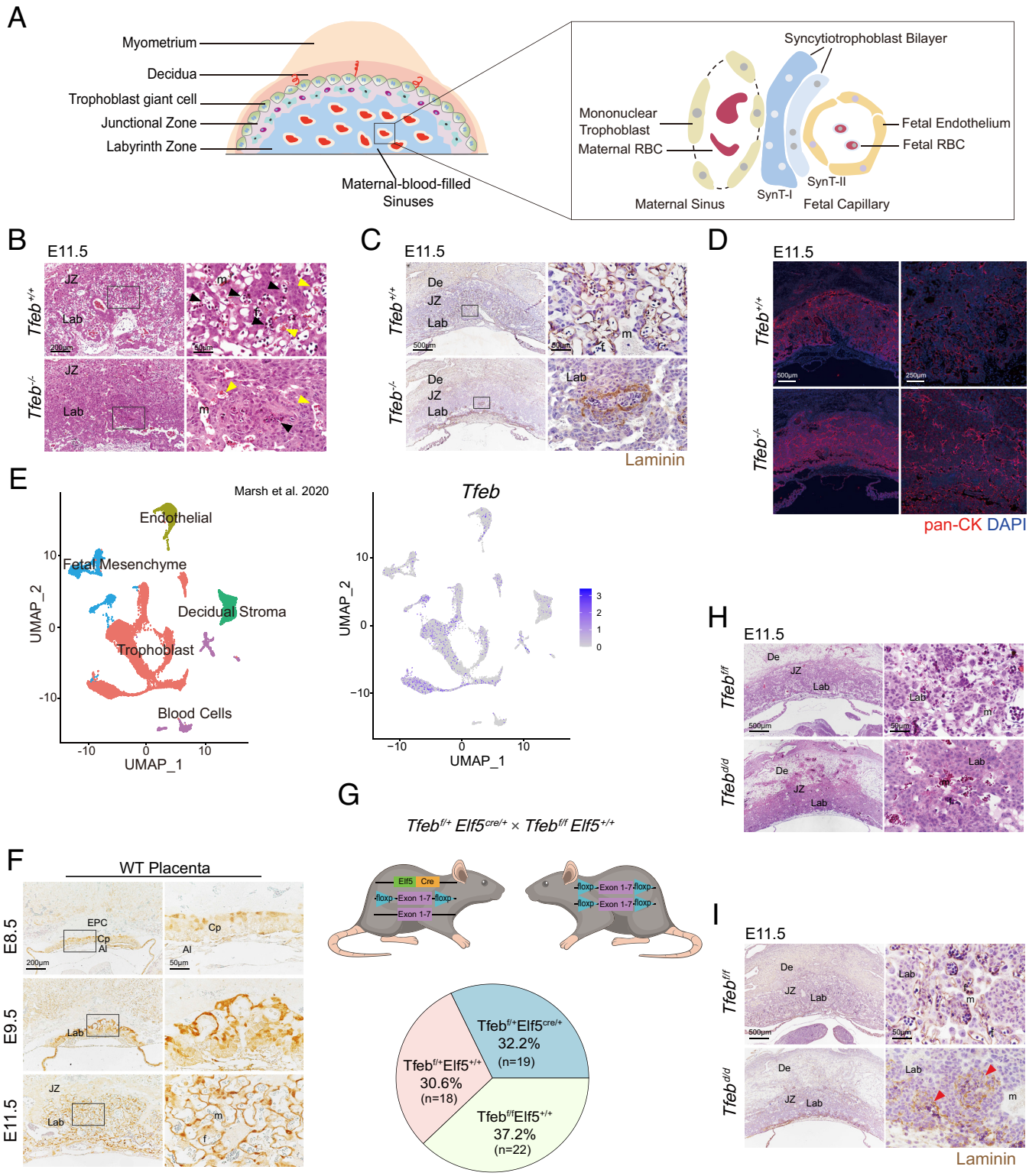

Fig. 5. Trophoblast-specific deletion of TFEB renders aberrant development of placental labyrinth. (*A*) Schematic diagram illustrating the structure and cell composition of mouse placenta. (*B–D*) Representative H&E (*B*), laminin (*C*), and pan-CK (*D*) staining of *Tfeb*$^{+/+}$ and *Tfeb*$^{-/-}$ placenta at E11.5. Black arrowhead, fetal capillary (f); yellow arrowhead, maternal sinus (m). Laminin is a marker of fetal blood vessel endothelium and pan-CK is a trophoblast marker. (*E*) *Tfeb* expression in different cell types illustrated by a single-cell atlas of WT mouse placenta using published snRNA-seq data. *Left* panel, the uniform manifold approximation and projection (UMAP) plot of major cell types in WT placentas. *Right* panel, UMAP plot displaying the distribution and relative *Tfeb* expression in different cell clusters. (*F*) Representative immunohistochemical images of Tfeb in mouse placentas. (*G*) Pie chart showing the proportion of live offsprings from trophoblast-specific TFEB KO mice. (*H* and *I*) Representative H&E stains (*H*) and immunohistochemical staining for laminin (*I*) of *Tfeb*$^{f/f}$ and *Tfeb*$^{d/d}$ placentas at E11.5. EPC, ectoplacental cone; De, decidua; Lab, labyrinth; Al, allantois; JZ, junctional zone; Cp, Chorionic plate.

fetal capillaries remained consistently undetectable (Fig. 5*F*). These observations suggest that the defective placental development in Tfeb mutant mice is directly caused by the deleterious effects of *Tfeb* deletion in labyrinth trophoblasts.

To further ascertain whether Tfeb functions in a trophoblast cell-autonomous manner to sustain placental and fetal development, we generated trophoblast-specific *Tfeb* KO mice (designated as *Tfeb*$^{d/d}$) by cross-breeding *Tfeb-flox* mice (*Tfeb*$^{f/f}$) with *Elf5-Cre* mice

(Fig. 5*G*). The successful *Tfeb* deletion specifically in trophoblasts was verified by immunohistochemistry staining (*SI Appendix,* Fig. S7*D*). Genotype examination of the live newborns at birth indicated that trophoblast-specific *Tfeb* deletion is sufficient to cause embryonic lethality (Fig. 5*G*). The yolk sac of $Tfeb^{d/d}$ mutants at E11.5 exhibited paleness and was devoid of blood vessel branching (*SI Appendix,* Fig. S7*E*), with concomitant diminished vascular networks in the corresponding placentas. In addition, $Tfeb^{d/d}$ conceptuses displayed severe fetal growth retardation and demise at E11.5 (*SI Appendix,* Fig. S7*F*), consistent with embryonic demise phenotypes in the $Tfeb^{-/-}$ mutants. H&E and Laminin staining revealed underdeveloped fetal vasculatures in the $Tfeb^{d/d}$ placenta (Fig. 5 *H* and *I*), fully recapitulating the phenotypes in systemic *Tfeb* null placentas. In summary, our findings suggest that the embryonic lethality phenotype identified in *Tfeb* KO mice is prominently attributed to the essential roles Tfeb plays in labyrinth trophoblast differentiation.

Tfeb Is Required for SynT-I Formation during Mouse Placental Development. To uncover how Tfeb signaling governs trophoblast differentiation, we performed RNA-seq analysis on the E9.5 and E11.5 placentas to define the transcriptome signature in *Tfeb* KO placentas. The RNA-seq data showed 22 up-regulated and 247 down-regulated genes in the E9.5 mutant placentas compared with controls, whereas 1,019 genes were down-regulated at E11.5 (Fig. 6*A* and *SI Appendix,* Fig. S8*A*). Gene set enrichment analysis on the down-regulated DEGs highlighted significant enrichment of genes associated with placental development and angiogenesis in *Tfeb* null placentas (*SI Appendix,* Fig. S8 *B* and *C*). Strikingly, we found robust downregulation of marker genes for SynT-I (including *Slc16a1*, *Tfrc*, *Tgfa*, and *Synа*) and SynT-II (*Gcm1* and *Slc16a3*) in KO placentas (Fig. 6*B*), while markers for TGCs and SpT showed no difference. qPCR of trophoblast markers confirmed these findings in both systemic and trophoblast-specific *Tfeb* KO placentas (*SI Appendix,* Fig. S8 *D* and *E*). Thus, we speculated that *Tfeb* ablation may predominantly obstruct the formation of the STBs.

To investigate whether Tfeb depletion leads to aberrant development in both STB lineages, SynT-I and SynT-II, we employed the snRNA-seq to verify the expression of *Tfeb* in STB bilayers. We noticed abundant *Tfeb* expression in SynT-I and SynT-I precursors, rather than in SynT-II and its corresponding precursors (Fig. 6 *C* and *D*). In addition, coimmunofluorescence for monocarboxylate transporter 1 (Mct1; a marker for SynT-I) and Tfeb clearly showed their precise colocalization (*SI Appendix,* Fig. S8*F*). Consistently, in situ hybridization (ISH) results demonstrated that in WT placentas *Tfeb* was coexpressed with *Synа*, the fusogen specifically regulating SynT-I formation, instead of the SynT-II gene *Gcm1* at E8.5 (*SI Appendix,* Fig. S8 *G* and *J*). Collectively, these data suggest that Tfeb may be uniquely required for the development of the SynT-I lineage.

To support this speculation, we intersected the top-down-regulated genes in E9.5 mutant placentas with the markers for different trophoblast subtypes. Strikingly, the most significantly repressed genes in KO placentas were predominantly enriched in the SynT-I precursor and SynT-I, rather than SynT-II and other trophoblast lineages, highlighting a more severe impact on the development of SynT-I (Fig. 6*D*). Remarkably, immunofluorescence staining further revealed the invariable disappearance of Mct1-positive SynT-I cells in E11.5 Tfeb global and conditional KO placentas, affirming that Tfeb is crucial for the differentiation of SynT-I (Fig. 6 *E* and *F*). In addition, transmission electron microscope images illustrated a single layer of STB and disorganized trophoblast cells in Tfeb-deficient placentas, contrasting with the STB bilayer structure in WT counterparts (*SI Appendix,* Fig. S8*H*). Although there were also partially diminished SynT-II cells present in *Tfeb* mutant placentas, we assumed that impaired SynT-II differentiation may be secondary to the underdifferentiated SynT-I, given the exclusive Tfeb expression in SynT-I cells. Indeed, double immunofluorescence staining for Mct1 and Mct4 revealed that E9.5 *Tfeb* KO placentas are completely devoid of SynT-I cells but preserving relatively normal SynT-II trophoblasts (*SI Appendix,* Fig. S8*I*), implying that the defective SynT-I formation in the *Tfeb* KO chorion predisposes the occurrence of disrupted SynT-II differentiation.

Given that the phenotype of compromised SynT-I formation in *Tfeb* mutant mice showed striking similarity with the $Synа^{-/-}$ placenta (33), we postulated that Tfeb deficiency might affect the expression of *Synа* in the process of SynT-I differentiation. ISH staining revealed that *Synа* mRNA disappeared from the chorion plate in *Tfeb* KO placentas (Fig. 6*G* and *SI Appendix,* Fig. S8*J*). Luciferase assay results illustrated that the *Synа* promoter sequence with CLEAR motifs responded to Tfeb overexpression (Fig. 6*H*). Collectively, evidence from KO mice identifies Tfeb as an essential regulator of SynT-I differentiation in vivo, the dysfunction of which results in a wide spectrum of trophoblast and vascular defects.

Elevated TFEB Expression Correlates with Augmented Trophoblast Syncytialization in Human FGR Placentas. Building upon our previous study, which unveiled a significant reinforcement of trophoblast syncytialization in response to nutrient scarcity and mTOR inhibition in FGR placentas (17), we next sought to explore whether TFEB is relevant to this phenotype. A comparative analysis of TFEB, SYNCYTIN2, and p-S6K (the mTORC1 activity hallmark) expression was conducted in FGR and healthy gestational age-matched control placentas (*SI Appendix,* Fig. S9*A*). Consistent with our previous findings (17), western blot analysis of p-S6K/S6K confirmed the suppression of mTORC1 signaling in FGR placentas (*SI Appendix,* Fig. S9 *A* and *B*). Concomitantly, elevated levels of TFEB and STB maker SYNCYTIN2 were observed in the FGR placentas by 80% and 70%, respectively (*SI Appendix,* Fig. S9 *A* and *B*). Statistical analysis further revealed a positive correlation between TFEB and SYNCYTIN2 expression, aligning with the regulatory influence of TFEB on *ERVFRD-1* (*SI Appendix,* Fig. S9*C*). Moreover, we verified more intense nuclear TFEB signals in the FGR placentas exhibiting excessive STBs as verified previously, particularly in the CTBs prone to fusion (*SI Appendix,* Fig. S9*D*). These results substantiate a close correlation between elevated TFEB activity and enhanced trophoblast syncytialization in response to nutrient insufficiency in FGR placentas, implying that TFEB is intricately associated with placental adaptation to nutrient insufficiency in FGR.

Discussion

In this study, we demonstrate comprehensively in cell and mouse experiments that TFEB acts as a key transcriptional factor that controls STB differentiation (Fig. 6*I*). In contrast to TFEB's canonical function as a master regulator of the autolysosomal pathway, TFEB confers direct transcriptional regulation of its target gene *ERVFRD-1* in human trophoblasts, thereby promoting trophoblast fusion. In mice, depleting *Tfeb* specifically in trophoblasts hinders the differentiation of STBs, most strikingly in the SynT-I lineage, leading to extensive placental defects and embryonic lethality. In summary, our findings underscore an autophagy-lysosomal pathway-independent function of TFEB in placenta development, which illuminates the mechanism underlying the

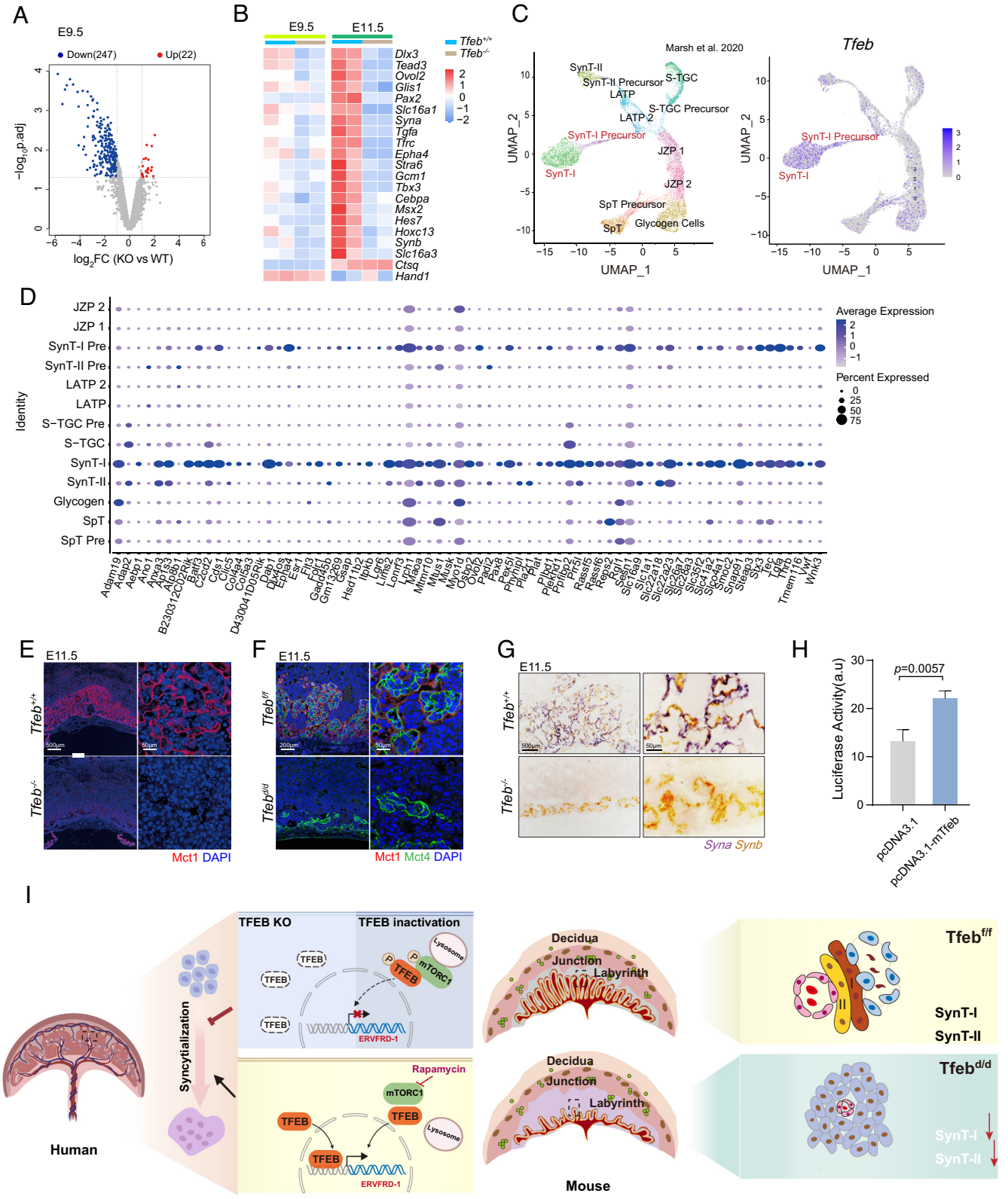

Fig. 6. Tfeb is required for SynT-I formation. (*A*) Volcano plot depicting DEGs identified by RNA-seq in E9.5 placentas ($Tfeb^{-/-}$ vs $Tfeb^{+/+}$). (*B*) Heatmap showing the expression of SynT-I and SynT-II markers in $Tfeb^{-/-}$ and $Tfeb^{+/+}$ placentas at E9.5 and E11.5. (*C*) UMAPs showing *Tfeb* expression in different trophoblast subtypes. (*D*) Dot plots illustrate the average expression and percentage of nuclei in each cluster in which DEGs were identified using DESeq2 with criteria as absolute $\log_2$ FC < −2, *P*adj. < 0.05 in E9.5. (*E* and *F*) Immunohistochemical staining for Mct1 and Mct4 illustrating the formation of SynT-I and SynT-II respectively in systemic *Tfeb* KO (*E*) and trophoblast-specific *Tfeb* KO mice (*F*). (*G*) ISH of *Syna* and *Synb* in $Tfeb^{+/+}$ and $Tfeb^{-/-}$ placentas. (*H*) Dual-luciferase reporter assays showing the activity of *Syna* promoter in response to exogenous *Tfeb* overexpression. HEK293T cells transfected with Syna promoter were cotransfected with pcDNA3.1-mTfeb or pcDNA3.1 as a control. (*I*) A working model of the TFEB-regulated trophoblast syncytialization during human and mouse placentation. The schematic in (*I*) was created using BioRender.

cross talk between placental development and nutrient-sensing machinery during pregnancy.

Trophoblast syncytialization is a finely orchestrated process that relies on transcriptional programming, membrane remodeling, and epigenetic and metabolic regulation (13, 14, 16, 34). We recently demonstrated that nutrient insufficiency and mTORC1 inhibition profoundly enhance the formation of placental syncytium, thereby counteracting nutrient scarcity stress to sustain fetal growth (17). However, there is no experimental evidence on how trophoblast transforms the mTORC1 nutrient signal into trophoblast differentiation response. Our study not only demonstrates the critical role of endogenous TFEB in sustaining proper trophoblast syncytialization under normal developmental conditions but also uncovers a coupling between TFEB activation and excessive trophoblast syncytialization in response to nutrient stress signaling. Besides mTORC1, other kinases, including ERK2, AMPK, AKT, and GSK3β, also control the phosphorylation and the intracellular localization of TFEB. In addition to phosphorylation, TFEB activity undergoes extensive regulation through various post-translational modifications, such as acetylation, ubiquitination, and SUMOylation (35). Consequently, any disruptions caused by these modifications in TFEB expression or activity, beyond responses to nutrient availability, such as those arising from lysosomal stress, transcriptional dysregulation, abnormal cytokine response, and hypoxia, could potentially impact STB differentiation and placental development via TFEB signaling. Moreover, we observed dynamic changes in TFEB RNA levels during the process of trophoblast syncytialization. Emerging evidence has shown that TFEB activity is controlled at the transcriptional level in a cell type–specific manner. Further investigation is required to understand the complex transcriptional regulation of TFEB in placentas.

Mechanistically, our study illustrates that the pro-syncytialization effects of TFEB are mediated through the transcriptional activation of trophoblast fusogens. TFEB canonically acts as a master transcriptional factor for autophagy and lysosomal biogenesis by driving the expression of critical autophagy and lysosome genes (25, 26). Recently, emerging evidence also highlights autophagy-lysosomal-independent roles of TFEB in various physiological and disease conditions (36–38). Here, our study identified that *ERVFRD-1* is a TFEB target gene governing trophoblast syncytialization and placenta development. In addition to TFEB, previous studies have shown that *ERVFRD-1* expression is also profoundly controlled by protein kinase A signaling and GCM1 in the trophoblast cell line (9). Nonetheless, we compared the relative contribution of GCM1 and TFEB to *ERVFRD-1* expression and confirmed that TFEB displayed much greater regulatory efficiency than GCM1, which highlights the importance of the TFEB signaling in STB differentiation. In addition, the consistent phenotypes of TFEB-mediated syncytialization and the similar transcriptional regulatory effect of TFEB on trophoblast fusogens both in humans and mice conceivably imply that this conserved gene regulation machinery for sustaining trophoblast syncytialization may be preserved over evolution as a fundamental mechanism beneficial for the development and function of hemochorial placentas.

Previous studies have shown that the homozygous *Tfeb* mutant is embryonic lethal, likely due to abnormal placental vascularization (30). Our study further expands on these findings and demonstrates that trophoblast-specific deletion of *Tfeb* is sufficient to fully recapitulate the phenotypes observed in whole-body KO mice. Given the exclusive Tfeb expression pattern in mouse STB lineages rather than endothelium, we propose that the aberrant STB formation is the primary cause of the embryonic lethality in *Tfeb* mutants. Unlike the single STB layer in human placentas, the interhemal membrane separating maternal and fetal blood compartments in the mouse labyrinth is constituted by two intimately juxtaposed layers of SynT-I and SynT-II (31). Accumulating studies have identified genes functionally important for SynT-II formation by leveraging genetically modified mouse models, including mutants of *Gcm1*, *Synb*, *Fzd5*, and *Tmem16f* (39–42). However, the molecular mechanisms underlying SynT-I differentiation are relatively limited and mostly speculative. Our current study provides strong experimental evidence supporting Tfeb's role as a SynT-I transcriptional factor. Notably, the *Tfeb* mutant phenotype closely resembles that of *Syna*, which serves as a bona fide fusogene governing mouse SynT-I development in cooperation with its receptor Ly6e. Given our finding that Tfeb could also directly promote the expression of *Syna*, we postulate that the Tfeb-Syna axis working in concert finetunes the transcriptional regulation of SynT-I formation, while it should be noted that the phenotypes in the Tfeb deficient placentas appear to be slightly more severe than the $Syna^{-/-}$ and $Ly6e^{-/-}$ mutants (33, 43). Nevertheless, we also observed impaired SynT-II formation in *Tfeb* KO placentas. Akin to the *Tfeb* mutants, previous studies revealed that the deletion of SynT-I-specific genes, including *Syna*, *Ly6e,* and *Atp11a*, is also accompanied by SynT-II destruction of variable severity. Our data showed that the defective SynT-I formation in *Tfeb* KO placentas was prior to the occurrence of SynT-II defects, which implies that SynT-II malformation is likely secondary to the SynT-I defects in *Tfeb* KO mice. Although recent evidence, especially from single-cell transcriptome analysis (32), suggests that SynT-I and SynT-II originate independently from their corresponding progenitors, our findings suggest the formation of these two adjacent STB layers seems to be mechanistically intertwined. The molecular mechanism underlying the interplay between these two layers required further investigation. Moreover, we identify Tfeb as a transcriptional factor governing SynT-I formation, which may also exert indirect impacts on organizing the development of vasculature networks in the mouse placenta. The molecular cross talk between trophoblasts and endothelium, such as Vegfa signaling mediated interactions, needs to be further studied under the condition of Tfeb deficiency.

We observed that elevated TFEB expression scale with the upregulation of the STB maker in human FGR placentas, which suggests that TFEB may be the key player driving the placental adaptation to nutrient insufficiency in FGR placentas. Moreover, impaired trophoblast syncytialization has been observed in preeclampsia placentas (44). Concomitantly, TFEB expression and its nuclear translocation were significantly reduced in preeclamptic trophoblasts (45). However, whether low TFEB expression also contributes to defective syncytium formation in preeclampsia and the corresponding mechanisms requires further investigation. The manipulation of the TFEB signaling may be of biomedical relevance for treating human pregnancy complications characterized by aberrant STB differentiation. Trehalose, a naturally occurring disaccharide, has recently gained extensive attention as a TFEB agonist to mitigate diseases related to lysosomal disorders (46). In the present study, we unveil a role of trehalose in reinforcing trophoblast syncytialization in vitro. Therefore, the in vivo function and clinical potential of trehalose treatment in pregnancy diseases merits further exploration.

In summary, our study uncovers an indispensable role of TFEB in human and mouse placenta development by regulating the transcription of trophoblast fusogens and safeguarding trophoblast syncytialization. This finding offers valuable insights into the interplay between cell signaling response to nutrient viability and trophoblast syncytialization, which opens broad avenues for studying placenta development and etiologies of pregnancy complications from the perspective of nutritional regulation.

Materials and Methods

Mice. All mouse studies were reviewed and approved by the Xiamen University Laboratory Animal Center (XMULAC20210168). The *Tfeb*-null mice (*Tfeb*$^{-/-}$; #T016716) and *Tfeb*$^{flox/flox}$ (*Tfeb*$^{f/f}$; #T015917) mice were generated by GemPharmatech Co., Ltd. Trophoblast-specific ablation of *Tfeb* was achieved by crossing *Tfeb*^{flox} mice with transgenic mice expressing Cre-recombinase driven by the *Elf5* promoter (*Elf5*-Cre), provided by Haibin Wang's lab at Xiamen University (47). *Tfeb*$^{f/+}$*Elf5*$^{cre/+}$ mice were mated with *Tfeb*$^{f/f}$*Elf5*$^{+/+}$ mice to generate offspring with a specific deletion of *Tfeb* in trophoblasts (referred to as *Tfeb*$^{d/d}$ mice). All mice used in this study were kept at C57BL6 background and maintained in a specific pathogen-free animal facility. For mating experiments, male and nulliparous female mice aged between 8 and 12 wk were cohoused, and embryonic day 0.5 (E0.5) of pregnancy was defined as the first observation of a vaginal plug. Mice were genotyped by PCR of genomic DNA extracted from tails or toes using the primers listed in *SI Appendix*, Table S1.

Human sample collection, cell culture and cell fusion, RNA interference and generation of CRISPR knock-out cell lines, molecular cloning and overexpression, Luciferase assay, immunoblot analysis, RNA extraction and qPCR, ChIP-seq, RNA seq, cell immunofluorescence staining, histology and immunostaining, ISH, ELISA, statistical analysis, and data availability.

The corresponding detailed protocols and information can be found in *SI Appendix, Materials and Methods*.

Data, Materials, and Software Availability. RNA-seq and ChIP-seq have been deposited in Gene Expression Omnibus (GEO accession no. GSE252254) (48).

ACKNOWLEDGMENTS. We thank Drs. Jason Mills at Baylor College of Medicine and Yang Zhang at Shenzhen Bay Laboratory for valuable comments and editing. We acknowledge Dr. Andrea Ballabio at Telethon Institute of Genetics and Medicine for technical support. This study was supported by grants from the National Key Research and Development Program of China (2022YFC2702400 to B.C. and Y.-L.W. and 2022YFC2704702 to X.H.), the National Natural Sciences Foundation in China (82130047 and 81971414 to B.C. and 82192872 to X.S.), the Natural Sciences Foundation of Fujian Province of China (2020J06003 to B.C.), NIH/NICHD grant (R01HD091218 to I.U.M.), Strategic Collaborative Research Program of the Ferring Institute of Reproductive Medicine, Ferring Pharmaceuticals, and Chinese Academy of Sciences (FIRMA200503 to B.C.).

Author affiliations: [a]Fujian Provincial Key Laboratory of Reproductive Health Research, Department of Obstetrics and Gynecology, Women and Children's Hospital, School of Medicine, Xiamen University, Xiamen 361102, Fujian, China; [b]State Key Laboratory of Infectious Disease Vaccine Development, Xiang An Biomedicine Laboratory, School of Public Health, Xiamen University, Xiamen 361102, Fujian, China; [c]State Key Laboratory of Stem Cell and Reproductive Biology, Institute of Zoology, Chinese Academy of Sciences, Beijing 100101, China; [d]University of Chinese Academy of Sciences, Beijing 100101, China; [e]Beijing Institute for Stem Cell and Regenerative Medicine, Beijing 100101, China; [f]Institute of Comparative Medicine, College of Veterinary Medicine, Yangzhou University, Yangzhou 225009, Jiangsu, China; [g]Guangdong Provincial Key Laboratory of Major Obstetric Diseases, Department of Obstetrics and Gynecology, The Third Affiliated Hospital of Guangzhou Medical University, Guangzhou 510140, Guangdong, China; [h]Guangdong Provincial Clinical Research Center for Obstetrics and Gynecology, The Third Affiliated Hospital of Guangzhou Medical University, Guangzhou 510140, Guangdong, China; [i]Department of Medicine, Section of Infectious Diseases, Baylor College of Medicine, Houston 77030, TX; and [j]Department of Molecular Virology and Microbiology, Baylor College of Medicine, Houston 77030, TX

Author contributions: Y.-L.W., X.H., and B.C. designed research; W.Z., Y.Z., P.X., Z.W., X.S., C.C., J.L., H.W., Y.-L.W., X.H., and B.C. performed research; H.C., F.L., X.Z., D.C., I.U.M., Y.-L.W., X.H., and B.C. contributed new reagents/analytic tools; W.Z., Y.Z., Y.W., M.S., W.D., H.W., X.H., and B.C. analyzed data; and W.Z., Y.Z., I.U.M., Y.-L.W., X.H., and B.C. wrote the paper.

1. M. Knofler *et al.*, Human placenta and trophoblast development: Key molecular mechanisms and model systems. *Cell Mol. Life Sci.* **76**, 3479–3496 (2019).
2. M. Y. Turco, A. Moffett, Development of the human placenta. *Development* **146**, dev163428 (2019).
3. G. J. Burton, A. L. Fowden, The placenta: A multifaceted, transient organ. *Philos. Trans. R. Soc. Lond. B Biol. Sci.* **370**, 20140066 (2015).
4. E. Maltepe, S. J. Fisher, Placenta: The forgotten organ. *Annu. Rev. Cell Dev. Biol.* **31**, 523–552 (2015).
5. P. Diaz, T. L. Powell, T. Jansson, The role of placental nutrient sensing in maternal-fetal resource allocation. *Biol. Reprod.* **91**, 82 (2014).
6. O. Farah, C. Nguyen, C. Tekkatte, M. M. Parast, Trophoblast lineage-specific differentiation and associated alterations in preeclampsia and fetal growth restriction. *Placenta* **102**, 4–9 (2020).
7. H. Zhou *et al.*, Regulators involved in trophoblast syncytialization in the placenta of intrauterine growth restriction. *Front Endocrinol. (Lausanne)* **14**, 1107182 (2023).
8. X. Lu *et al.*, Fine-tuned and cell-cycle-restricted expression of fusogenic protein syncytin-2 maintains functional placental syncytia. *Cell Rep.* **23**, 3979 (2018).
9. S. J. Renaud, M. J. Jeyarajah, How trophoblasts fuse: An in-depth look into placental syncytiotrophoblast formation. *Cell Mol. Life Sci.* **79**, 433 (2022).
10. F. Mallet *et al.*, The endogenous retroviral locus ERVWE1 is a bona fide gene involved in hominoid placental physiology. *Proc. Natl. Acad. Sci. U.S.A.* **101**, 1731–1736 (2004).
11. S. Blaise, N. de Parseval, L. Benit, T. Heidmann, Genomewide screening for fusogenic human endogenous retrovirus envelopes identifies syncytin 2, a gene conserved on primate evolution. *Proc. Natl. Acad. Sci. U.S.A.* **100**, 13013–13018 (2003).
12. S. Mi *et al.*, Syncytin is a captive retroviral envelope protein involved in human placental morphogenesis. *Nature* **403**, 785–789 (2000).
13. J. D. Aplin, C. J. P. Jones, Cell dynamics in human villous trophoblast. *Hum. Reprod. Update* **27**, 904–922 (2021).
14. M. A. Costa, Scrutinising the regulators of syncytialization and their expression in pregnancy-related conditions. *Mol. Cell. Endocrinol.* **420**, 180–193 (2016).
15. S. K. Gupta, S. S. Malhotra, A. Malik, S. Verma, P. Chaudhary, Cell signaling pathways involved during invasion and syncytialization of trophoblast cells. *Am. J. Reprod. Immunol.* **75**, 361–371 (2016).
16. M. Yu *et al.*, Endogenous retrovirus-derived enhancers confer the transcriptional regulation of human trophoblast syncytialization. *Nucleic Acids Res.* **51**, 4745–4759 (2023).
17. X. Shao *et al.*, Placental trophoblast syncytialization potentiates macropinocytosis via mTOR signaling to adapt to reduced amino acid supply. *Proc. Natl. Acad. Sci. U.S.A.* **118**, e2017092118 (2021).
18. R. Puertollano, S. M. Ferguson, J. Brugarolas, A. Ballabio, The complex relationship between TFEB transcription factor phosphorylation and subcellular localization. *EMBO J.* **37**, e98804 (2018).
19. G. Napolitano, A. Ballabio, TFEB at a glance. *J. Cell Sci.* **129**, 2475–2481 (2016).
20. A. Tan, R. Prasad, C. Lee, E. H. Jho, Past, present, and future perspectives of transcription factor EB (TFEB): Mechanisms of regulation and association with disease. *Cell Death Differ.* **29**, 1433–1449 (2022).
21. H. Okae *et al.*, Derivation of human trophoblast stem cells. *Cell Stem Cell* **22**, 50–63.e56 (2018).
22. T. Shimizu *et al.*, CRISPR screening in human trophoblast stem cells reveals both shared and distinct aspects of human and mouse placental development. *Proc. Natl. Acad. Sci. U.S.A.* **120**, e2311372120 (2023).
23. C. Settembre *et al.*, A lysosome-to-nucleus signalling mechanism senses and regulates the lysosome via mTOR and TFEB. *EMBO J.* **31**, 1095–1108 (2012).
24. K. L. Carey *et al.*, TFEB transcriptional responses reveal negative feedback by BHLHE40 and BHLHE41. *Cell Rep.* **33**, 108371 (2020).
25. C. Settembre *et al.*, TFEB links autophagy to lysosomal biogenesis. *Science* **332**, 1429–1433 (2011).
26. M. Sardiello *et al.*, A gene network regulating lysosomal biogenesis and function. *Science* **325**, 473–477 (2009).
27. N. Singh *et al.*, Antimycobacterial effect of IFNG (interferon gamma)-induced autophagy depends on HMOX1 (heme oxygenase 1)-mediated increase in intracellular calcium levels and modulation of PPP3/calcineurin-TFEB (transcription factor EB) axis. *Autophagy* **14**, 972–991 (2018).
28. C. Esnault *et al.*, A placenta-specific receptor for the fusogenic, endogenous retrovirus-derived, human syncytin-2. *Proc. Natl. Acad. Sci. U.S.A.* **105**, 17532–17537 (2008).
29. C. Y. Liang *et al.*, GCM1 regulation of the expression of syncytin 2 and its cognate receptor MFSD2A in human placenta. *Biol. Reprod.* **83**, 387–395 (2010).
30. E. Steingrimsson, L. Tessarollo, S. W. Reid, N. A. Jenkins, N. G. Copeland, The bHLH-Zip transcription factor Tfeb is essential for placental vascularization. *Development* **125**, 4607–4616 (1998).
31. M. Hemberger, C. W. Hanna, W. Dean, Mechanisms of early placental development in mouse and humans. *Nat. Rev. Genet.* **21**, 27–43 (2020).
32. B. Marsh, R. Blelloch, Single nuclei RNA-seq of mouse placental labyrinth development. *Elife* **9**, e60266 (2020).
33. A. Dupressoir *et al.*, Syncytin-A knockout mice demonstrate the critical role in placentation of a fusogenic, endogenous retrovirus-derived, envelope gene. *Proc. Natl. Acad. Sci. U.S.A.* **106**, 12127–12132 (2009).
34. R. M. Mahr *et al.*, Mitochondrial citrate metabolism and efflux regulate BeWo differentiation. *Sci. Rep.* **13**, 7387 (2023).
35. M. Takla, S. Keshri, D. C. Rubinsztein, The post-translational regulation of transcription factor EB (TFEB) in health and disease. *EMBO Rep.* **24**, e57574 (2023).
36. B. Franco-Juarez *et al.*, TFEB; Beyond its role as an autophagy and lysosomes regulator. *Cells* **11**, 3153 (2022).
37. A. Tan, R. Prasad, E. H. Jho, TFEB regulates pluripotency transcriptional network in mouse embryonic stem cells independent of autophagy-lysosomal biogenesis. *Cell Death Dis.* **12**, 343 (2021).
38. N. Pastore *et al.*, TFEB regulates murine liver cell fate during development and regeneration. *Nat. Commun.* **11**, 2461 (2020).
39. J. Lu *et al.*, A positive feedback loop involving Gcm1 and Fzd5 directs chorionic branching morphogenesis in the placenta. *PLoS Biol.* **11**, e1001536 (2013).
40. L. Anson-Cartwright *et al.*, The glial cells missing-1 protein is essential for branching morphogenesis in the chorioallantoic placenta. *Nat. Genet.* **25**, 311–314 (2000).
41. A. Dupressoir *et al.*, Syncytin-A and syncytin-B, two fusogenic placenta-specific murine envelope genes of retroviral origin conserved in Muridae. *Proc. Natl. Acad. Sci. U.S.A.* **102**, 725–730 (2005).
42. Y. Zhang *et al.*, TMEM16F phospholipid scramblase mediates trophoblast fusion and placental development. *Sci. Adv.* **6**, eaba0310 (2020).
43. M. Hughes, B. V. Natale, D. G. Simmons, D. R. Natale, Ly6e expression is restricted to syncytiotrophoblast cells of the mouse placenta. *Placenta* **34**, 831–835 (2013).
44. C. S. Roland *et al.*, Morphological changes of placental syncytium and their implications for the pathogenesis of preeclampsia. *Cell Mol. Life Sci.* **73**, 365–376 (2016).
45. A. Nakashima *et al.*, Evidence for lysosomal biogenesis proteome defect and impaired autophagy in preeclampsia. *Autophagy* **16**, 1771–1785 (2020).
46. M. Khalifeh, G. E. Barreto, A. Sahebkar, Trehalose as a promising therapeutic candidate for the treatment of Parkinson's disease. *Br J. Pharmacol.* **176**, 1173–1189 (2019).
47. S. Kong *et al.*, Generation of Elf5-Cre knockin mouse strain for trophoblast-specific gene manipulation. *Genesis* **56**, e23101 (2018).
48. W. Zheng, Y. Zhang, TFEB safeguards trophoblast syncytialization in humans and mice. NCBI GEO. https://www.ncbi.nlm.nih.gov/geo/query/acc.cgi?acc=GSE252254. Deposited 31 December 2023.